Optics Letters

Mid-infrared supercontinuum generation in an all-fiberized Er-doped ZBLAN fiber amplifier

KAIXIN DENG,[1,†] LINYONG YANG,[1,2,3,†] BIN ZHANG,[1,2,3,4] JINMEI YAO,[1] AND JING HOU[1,2,3,5]

[1]College of Advanced Interdisciplinary Studies, National University of Defense Technology, Changsha 410073, China
[2]State Key Laboratory of Pulsed Power Laser Technology, Changsha 410073, China
[3]Hunan Provincial Key Laboratory of High Energy Laser Technology, Changsha 410073, China
[4]e-mail: nudtzhb@163.com
[5]e-mail: houjing25@sina.com

Received 11 September 2020; revised 9 October 2020; accepted 12 October 2020; posted 13 October 2020 (Doc. ID 409797); published 24 November 2020

A high power mid-infrared (MIR) supercontinuum (SC) is demonstrated in a strictly all-fiberized Er-doped ZBLAN fiber amplifier (EDZFA). The EDZFA is seeded by a 2.0–3.5 μm fiber-based SC laser and pumped at 976 nm. At pulse repetition rate of 500 kHz, the output SC spanning from 2.7 to 4.2 μm reaches a record output power of 4.96 W with an overall slope efficiency of 17.3%. This Letter, to the best of our knowledge, demonstrates the first all-fiberized in-amplifier SC generation in the MIR region, which has significant potential for further power scaling. © 2020 Optical Society of America

https://doi.org/10.1364/OL.409797

Fiber-based supercontinuum (SC) lasers find many applications in the biomedicine [1], spectroscopy [2], and defense and security [3] fields owing to its broad spectrum and good beam quality, as well as the robust and flexible design. SC generation in the 3–5 μm band, known as mid-infrared (MIR) region, is particularly attractive, since this wave band covers both the atmospheric transmission window and fundamental molecular absorption region, enabling gas detection [4] and hyperspectral measurement [5] applications. Since silica fibers suffer from limited transmission above 2.5 μm, non-silica fibers with lower phonon energy, such as fluoride (e.g., ZBLAN [6]), telluride [7], and chalcogenide [8] fibers, have been developed to extend the SC laser spectrum into the MIR region. Among them, ZBLAN fibers benefit from mature fabrication, relatively high damage threshold, and low phonon energy, and thus have been the most successful material in the demonstration of MIR SC generation.

A typical method to generate MIR SC in a fiber-based system is injecting high peak-power near-infrared pulses into undoped nonlinear fibers to enable spectral broadening. Researches based on this method have achieved a power up to 20.6 W with spectra spanning from 1.9 μm to 4.3 μm [6]. However, a significant drawback of this technique is low SC power ratio beyond 3 μm. Since the seed wavelength (usually 1.55 μm or 2 μm) is relatively far from the MIR region, most works present only 15%–20% of the total SC power distributed in the 3–5 μm band [9], with a large portion of energy not converted to the MIR region. Recently, higher power percentage above 3 μm (50%–60%) has been reported [10,11], but further improvement would be a challenge.

Another approach named in-amplifier MIR SC generation was proposed by Gauthier *et al.* [12,13], which is based on rare-Earth ion-doped fluoride fiber amplifiers. In Ref. [12], a 2.6–4.1 μm SC with a maximum output power of 154 mW was directly generated in an Er-doped ZBLAN fiber amplifier (EDZFA) seeded by an optical parametric generator (OPG) at 2.75 μm, which is much closer to the 3–5 μm band than 1.55 μm or 2 μm. In 2018, the output SC power obtained in EDZFA achieved watt-level [14] with a spectrum covering 2.7–4.25 μm. Recently Ho-doped ZBLAN fiber amplifiers were also investigated, since the gain band of Ho^{3+} is at 3 μm band. A SC spanning from 2.8 to 3.9 μm with a maximum output power of 411 mW has been reported [15]. The in-amplifier SC generation approach not only benefits from convenient configuration that directly generates SC in MIR region, but also shows competitiveness in high conversion ratio beyond 3 μm (usually above 70% [12–15]), thus having been considered as a promising scheme to improve the SC power distribution in 3–5 μm band.

However, current in-amplifier MIR SC generation is restricted to free-space coupling configuration, which loses the flexibility and stability of fiber-based systems. The poor launching efficiency results in thermal damage of fiber tips, and the reflections from surfaces of the lens may contribute to the parasitic lasing, which confines the power scaling of amplifiers [13]. Therefore, the output power is usually limited to hundreds of milliwatts [12,13,15]. To date, the highest output power of in-amplifier MIR SC is 1.75 W [14]. For further power scaling, an all-fiber design is required. Unfortunately, it is difficult to achieve all-fiber configuration for fluoride fiber amplifiers due to the unavailability of pump/signal fiber combiners in the MIR region. The only work [16] that achieved an all-fiberized ZBLAN fiber amplifier was based on a Ho-doped ZBLAN fiber amplifier, but the output SC spectrum range was 2.03–2.9 μm. To extend the spectrum to the MIR band, the amplifier was further cascaded to an undoped ZBLAN fiber, which still relies on

lens coupling. To the best of our knowledge, there are no reports on MIR SC generation in all-fiberized fluoride fiber amplifiers.

In this Letter, we report the first all-fiberized EDZFA, achieved by a novel design enabling direct fusion splicing from the seed and pump to the Er-doped ZBLAN fiber (EDZF). The all-fiber system produces a SC spanning from 2.7 to 4.2 μm with a maximum average output power of 4.96 W, a great increase compared to previous reports. Such a SC source is of considerable interest for long-term stability and power scaling.

The MIR SC generation setup is presented in Fig. 1, which consists of a 2–2.5 μm seed laser, a piece of undoped ZBLAN fiber, and an EDZFA. The structure of the broadband seed laser is similar to what we reported recently [17]. A 1550 nm pulsed laser provides 1 ns seed pulses at a variable repetition rate between 300 kHz and 500 kHz, which are pre-amplified in a dual-stage erbium-ytterbium-doped fiber amplifier (EYDFA) chain, frequency shifted to 2 μm band in a piece of single-mode fiber (SMF), and further amplified in a thulium-doped fiber amplifier (TDFA). Output SC pulses spanning from 2 to 2.5 μm are obtained after TDFA. These pulses are injected into a 10 m long undoped ZBLAN double-clad fiber (DCF) for further spectral broadening to cover the gain band of Er^{3+} at ∼2.75 − 2.85 μm, which is necessary for efficiently seeding the EDZFA. The core/cladding diameter and the corresponding NA of the undoped ZBLAN DCF are 12/125 μm and 0.23/0.40, respectively.

Then, the 2.0–3.5 μm seed pulses after the undoped ZBLAN fiber are launched into an EDZF for amplification. The 8.5 m long 7 mol.% double-cladding EDZF has a core with diameter of 15 μm and NA of 0.12, ensuring single-mode operation above 2.4 μm. Its inner cladding has a circular diameter of 260 μm truncated by two parallel flats separated by 240 μm, with a cladding absorption coefficient of ∼3 dB/m at 976 nm. A high concentration of Er^{3+} is chosen to enhance the energy transfer upconversion process ($^4I_{13/2}$, $^4I_{13/2} \rightarrow {}^4I_{15/2}$, $^4I_{9/2}$) and improves the gain of EDZFA.

The EDZFA is pumped at 976 nm via a $(2+1)\times 1$ signal/pump combiner by two 27 W laser diodes pigtailed to 105/125 μm, 0.22 NA silica fibers. The signal fiber port of the combiner is a DCF the same as the output fiber of TDFA, with a core/cladding diameter of 10/130 μm and core NA of 0.15. About 58% of the pump power was detected after the undoped ZBLAN DCF. Since an efficient combiner was used and a low-loss fusion splice (FS1) was obtained in our experiment, we suggest that the transmission loss of the ZBLAN fiber is mostly responsible for the decrease of pump power, which is also evidenced by the weak green fluorescence observed along the whole length of the undoped ZBLAN fiber.

A fusion splice joint (FS2) between the undoped ZBLAN fiber and the EDZF was achieved using method mentioned in Ref. [17]. The splicing process of FS2 was challenging since the cladding diameters of these two fibers (125 μm and 240 ∗ 260 μm, respectively) have large difference (see the inset image of FS2 in Fig. 1). Still, the transmission of FS2 reached 71%, which was measured using a 2000 nm continuous wave (CW) laser. Such a high seed launching efficiency is a significant improvement compared to that of free-space coupling (usually of ∼15%) in previous works [12–15]. This fusion splicing enables efficient coupling and mitigates the heat accumulation of the input end of EDZF, thus greatly enhancing the stability and power performance of the EDZFA.

An endcap made of multimode AlF_3 fiber ($L \approx 380$ μm) was spliced to the output end of the EDZF to protect the fiber tip from thermal damage at high powers. It was angle-cleaved to prevent parasitic lasing in the EDZFA. A cladding mode stripper (CMS) was fabricated to evacuate the unabsorbed pump light by recoating a section of the EDZF with high index polymer ($n = 1.64$). The EDZF was passively cooled on an aluminum plate filled with liquid coolant, and the output end of EDZF was secured in v-grooves.

The output average power of SC was monitored with a wavelength-insensitive thermopile power meter, and the spectrum at different pump powers was measured by a grating-based monochromator coupled to a liquid-nitrogen-cooled InSb detector. A long-pass filter with a cutoff wavelength of 3.6 μm was added to prevent the second-order grating diffraction when we measured the spectral components of longer wavelengths. The power ratio of the output SC beyond 3 μm was measured with a long-pass dichroic mirror (DM) having high transmission in 3–5 μm.

In the experiment, the signal pulse repetition rate (PRR) was first set to 300 kHz. The output spectra with respect to the launched pump power after FS2 are shown in Fig. 2(a). As expected, at low pump powers, the spectral component around 2.8 μm is amplified first. With the increasing of pump power, the output spectra broaden toward longer wavelengths. Such an asymmetrical spectral broadening is mainly caused by Raman soliton self-frequency shift (SSFS), a typical nonlinear effect in anomalous regime, since the zero dispersion wavelength (ZDW) of the fiber (1.65 μm) is far below the seed wavelengths. At sufficiently high pump powers, the amplified pulses around 2.8 μm break into multiple solitonic sub-components and then

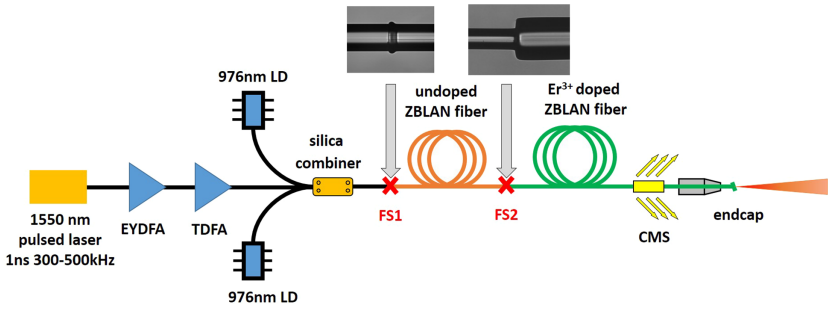

Fig. 1. Experimental setup of the mid-infrared supercontinuum generation in an all-fiberized Er-doped ZBLAN fiber amplifier. Inset, microscope images of the fusion splices (FS1-FS2). EYDFA, erbium-ytterbium-doped fiber amplifier; TDFA, thulium-doped fiber amplifier; LD, laser diode; FS1–FS2, fusion splices; CMS, cladding-mode stripper.

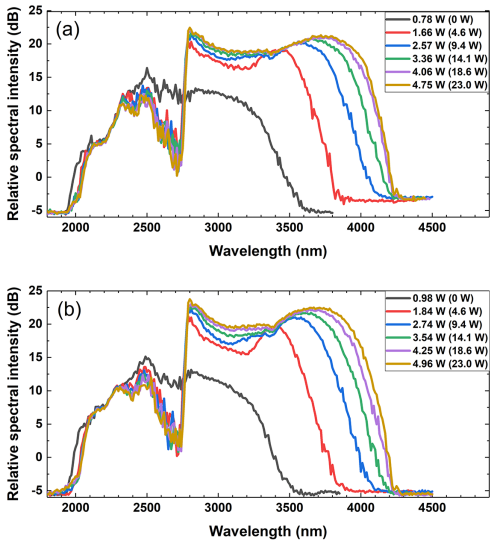

Fig. 2. Spectral evolution under signal PRR of (a) 300 kHz and (b) 500 kHz at different output powers. Corresponding launched pump powers are shown in parentheses.

shift to longer wavelengths due to SSFS. At the maximum pump power of 23.0 W, a 4.75 W SC spanning from 2.7 to 4.2 μm was obtained. However, one can observe a small peak at 2.8 μm for the 4.75 W curve corresponding to a parasitic CW lasing in EDZFA. The CW lasing, observed at a pump power threshold of ∼20.8 W, suppresses the amplification of the seed pulses, limiting further power scaling and spectral broadening of the EDZFA.

To improve the power performance of the EDZFA, we set the signal PRR to 500 kHz, and the output spectral revolution is depicted in Fig. 2(b). Similar asymmetrical spectral broadening was observed under PRR of 500 kHz. Although the spectra were not as broad as that under PRR of 300 kHz for lower pump powers, at maximum launched pump power of 23.0 W, the output power reaches 4.96 W with a spectrum from 2.7 to 4.2 μm. To the best of our knowledge, this is the highest SC power directly generated in a rare-Earth ion-doped fluoride fiber amplifier. The parasitic lasing threshold under PRR of 500 kHz also increases to ∼23.0 W, and the spectrum was still extending to longer wavelengths at the maximum power.

To evaluate the power characteristics of the EDZFA at different PRRs, the average output power of SC with respect to the launched pump power was measured, and the results are shown in Fig. 3. The efficiency achieves ∼19% for PRRs of both 300 kHz and 500 kHz at low pump powers (0–9.4 W), and slowly decreases when pump powers go higher. The whole slope efficiency of EDZFA was 17.2% at 300 kHz and 17.3% at 500 kHz. The slight difference indicates that the two PRRs are both high enough for the seed to extract the available gain in the amplifier, resulting in both relative high slope efficiencies. Further improvement in the efficiency of EDZFA could be expected, given that optimized fusion splices and endcaps are achieved and a more efficient thermal management is taken. The inset figure is a beam profile measured by a MIR camera, which shows the EDZFA operates at fundamental mode.

The percentage of SC power beyond 3 μm as a function of launched pump power is depicted in Fig. 4. Since it is difficult for a grating monochromator to precisely measure the spectral

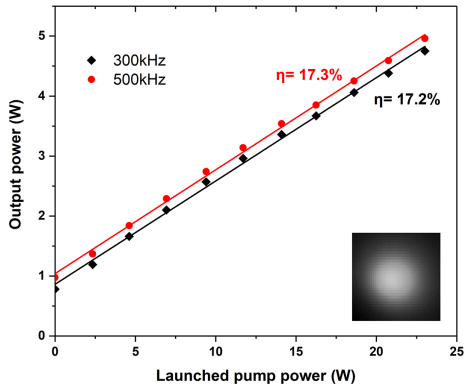

Fig. 3. Average output power of SC as a function of the launched pump power under different signal PRRs. Inset, beam profile of the output SC.

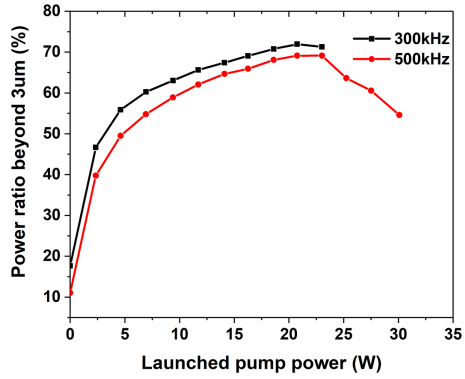

Fig. 4. Power percentage of the SC beyond 3 μm with increasing launched pump power at PRR of 300 kHz and 500 kHz.

intensity of parasitic lasing at 2.8 μm due to the limited spectral resolution, using the spectral integration method to calculate the power ratio above 3 μm may be imprecise. In our experiment, the SC power >3 μm was directly measured by a long-pass DM mentioned above. As is shown, for PRR of 300 kHz, the power ratio above 3 μm rises rapidly and exceeds 60% with the pump power increasing from 0 W to 6.93 W, and achieves the maximum of 71.9% at a pump power of 20.8 W. However, the percentage drops to 71% when the pump is further increased to 23.0 W, while corresponding spectra [Fig. 2(a)] show that CW lasing builds up at 2.8 μm and suppresses the spectral broadening. For PRR of 500 kHz, the power ratio beyond 3 μm reaches the maximum of 69.1% at launched pump power of 23.0 W. Further measurement for higher pump powers from 23 W to 30 W at 500 kHz shows that after the CW lasing occurs, the power beyond 3 μm maintains at ∼3.4 W, indicating that most of the increasing pump power was converted to the power of parasitic lasing. Owing to such a CW lasing, the power ratio beyond 3 μm decreases sharply from 69.1% to 54.6%, and the SC spectra were prevented from any broadening.

Table 1 presents a summary of previously reported MIR SC obtained from ZBLAN fiber amplifiers. It can be seen that the EDZFA in this report is the first all-fiberized ZBLAN fiber amplifier operating at MIR region. The novel all-fiber design greatly improves the overall robustness and stability of the

Table 1. Overview of MIR SC Generation in ZBLAN Fiber Amplifiers[a]

Seed Source Parameters	Gain Fiber Parameters	Coupling Technique	SC Characteristics		References
			Average Power	Spectral Range	
OPG, 2.75 μm, 400 ps, 2 kHz	Er: ZBLAN, 16/250 μm	lens coupling	154 mW	2.6–4.1 μm	[12]
OPG, 2.75 μm, 400 ps, 20 kHz	Er: ZBLAN, 16/250 μm	lens coupling	485 mW	2.7–4.0 μm	[13]
TDFA + GCF, 2.2–3.1 μm, 1.6 ns, 70 kHz	Er: ZBLAN, 16/250 μm	lens coupling	1.75 W	2.7–4.25 μm	[14]
TDFA + GCF, 2.4–3.2 μm, 1.6 ns, 50 kHz	Ho: ZBLAN, 10/125 μm	lens coupling	411 mW	2.8–3.9 μm	[15]
TDFA + ZBLAN, 2.0–3.5 μm, 1 ns, 500 kHz	Er: ZBLAN, 16/250 μm	**fusion splicing**	4.96 W	2.7–4.2 μm	This work

[a]OPG, optical parametric generator; TDFA, thulium-doped fiber amplifier; GCF, germania-core fiber.

EDZFA, and generates a record power of 4.96 W. We believe that by eliminating possible free-space reflections, this configuration also contributes to the high parasitic lasing threshold in our experiment (~23.0 W at 500 kHz).

In conclusion, we demonstrate an all-fiberized EDZFA generating a high-power SC spanning from 2.7 to 4.2 μm. The SC source delivers a record average power of 4.96 W, a significant improvement compared to previous reports. The strictly all-fiberized configuration enables the system to operate at high average power with excellent long-term stability. To the best of our knowledge, this is the first time that an in-amplifier MIR SC is obtained from an all-fiberized configuration, which also achieves the highest SC power generated in ZBLAN fiber amplifiers. Future work to improve the system includes optimizing the fusion splices and endcap, as well as increasing the PRR of the signal laser in an appropriate range. These are important for raising the parasitic lasing threshold and the further power scaling of SC. Replacing the current erbium-doped ZBLAN fiber with an erbium-doped InF_3 fiber can also be considered to extend the long wavelength edge of SC to 5 μm. Our all-fiber design is a promising approach opening new possibilities for efficient and high-power SC generation beyond 3 μm.

Funding. State Key Laboratory of Pulsed Power Laser Technology (SKL2020ZR06).

Disclosures. The authors declare no conflicts of interest.

[†]These authors contributed equally to this Letter.

REFERENCES

1. A. Labruyère, A. Tonello, V. Couderc, G. Huss, and P. Leproux, Opt. Fiber Technol. **18**, 375 (2012).
2. F. Borondics, M. Jossent, C. Sandt, L. Lavoute, D. Gaponov, A. Hideur, P. Dumas, and S. Fevrier, Optica **5**, 378 (2018).
3. A. Mukherjee, S. Von der Porten, and C. K. N. Patel, Appl. Opt. **49**, 2072 (2010).
4. D. Grassani, E. Tagkoudi, H. Guo, C. Herkommer, F. Yang, T. J. Kippenberg, and C.-S. Bres, Nat. Commun. **10**, 1553 (2019).
5. T. Hakala, J. Suomalainen, S. Kaasalainen, and Y. W. Chen, Opt. Express **20**, 7119 (2012).
6. L. Yang, B. Zhang, X. He, K. Deng, S. Liu, and J. Hou, J. Lightwave Technol. **38**, 5122 (2020).
7. C. Yao, Z. Jia, Z. Li, S. Jia, Z. Zhao, L. Zhang, Y. Feng, G. Qin, Y. Ohishi, and W. Qin, Optica **5**, 1264 (2018).
8. C. R. Petersen, U. Moller, I. Kubat, B. B. Zhou, S. Dupont, J. Ramsay, T. Benson, S. Sujecki, N. Abdel-Moneim, Z. Q. Tang, D. Furniss, A. Seddon, and O. Bang, Nat. Photonics **8**, 830 (2014).
9. J. Swiderski, Prog. Quantum Electron. **38**, 189 (2014).
10. J. Swiderski and M. Michalska, Opt. Lett. **39**, 910 (2014).
11. K. Yin, B. Zhang, L. Yang, and J. Hou, Opt. Lett. **42**, 2334 (2017).
12. J.-C. Gauthier, V. Fortin, S. Duval, R. Vallée, and M. Bernier, Opt. Lett. **40**, 5247 (2015).
13. J.-C. Gauthier, L.-R. Robichaud, V. Fortin, R. Vallée, and M. Bernier, Appl. Phys. B **124**, 122 (2018).
14. L. Yang, B. Zhang, T. Wu, Y. Zhao, and J. Hou, Opt. Lett. **43**, 3061 (2018).
15. L. Yang, B. Zhang, K. Yin, T. Wu, Y. Zhao, and J. Hou, Photon. Res. **6**, 417 (2018).
16. L. Yang, B. Zhang, K. Yin, Y. Zhao, and J. Hou, J. Lightwave Technol. **36**, 3193 (2018).
17. L. Yang, B. Zhang, D. Jin, T. Wu, X. He, Y. Zhao, and J. Hou, Opt. Lett. **43**, 5206 (2018).